Expanded View Figures

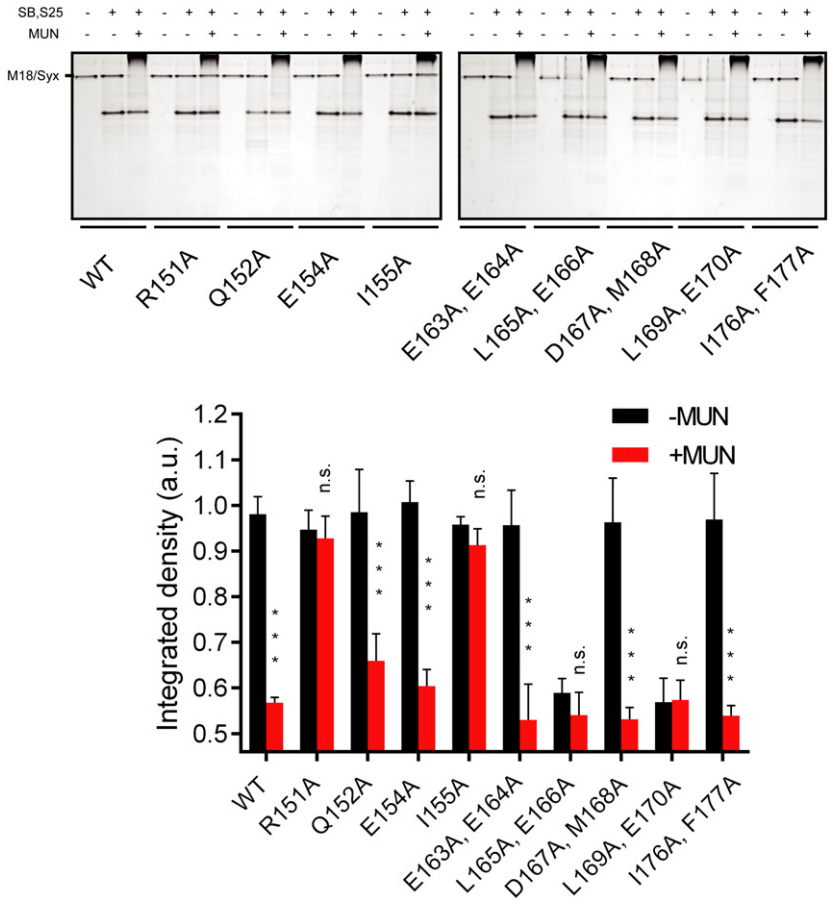

Figure EV1. Relative ternary SNARE complex formation bearing the syntaxin-1 linker region mutations in the presence of Munc18-1 and/or the MUN domain as monitored by native gel electrophoresis.

Integrated intensities of the bands of the Munc18-1/syntaxin-1 (M18/Syx) complex were used to determine relative ternary SNARE complex formation: The band of the M18/Syx complex gradually disappears with ternary SNARE complex formation in the presence of SNAP-25, synaptobrevin-2, and the MUN domain. The upper panel shows representative Coomassie brilliant blue-stained native electrophoresis gels from one of three independent experiments. Data are processed by ImageJ (NIH) and shown as means ± SEM; n.s., not significant ($P > 0.05$); ***$P < 0.001$, using Student's *t*-test with $n = 3$ technical replicates.

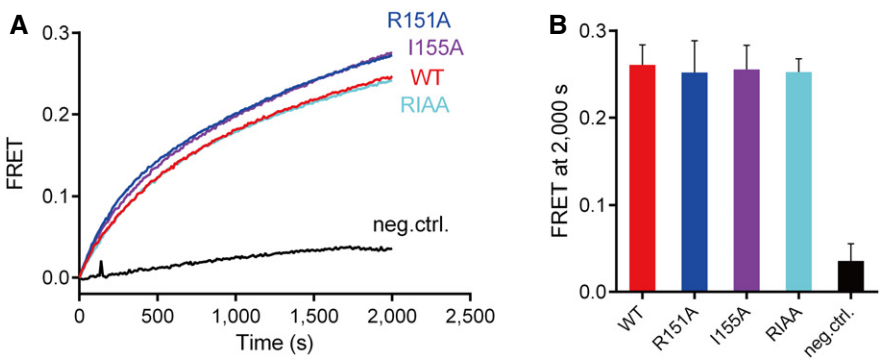

Figure EV2. The R151A, I155A mutations of syntaxin-1 have no effect on ternary SNARE complex formation with syntaxin-1, SNAP-25, and synaptobrevin-2 (i.e. in the absence of Munc18-1 and the MUN domain).

A, B Ternary SNARE complex formation as monitored by ensemble FRET efficiency between fluorescent dye-labeled SNAP-25 and the cytoplasmic domain of synaptobrevin-2 (A) and quantification of the results (B). Neg. ctrl. (negative control): The experiment was performed in the absence of syntaxin-1. Shown are means ± SD for $n = 3$ technical replicates.

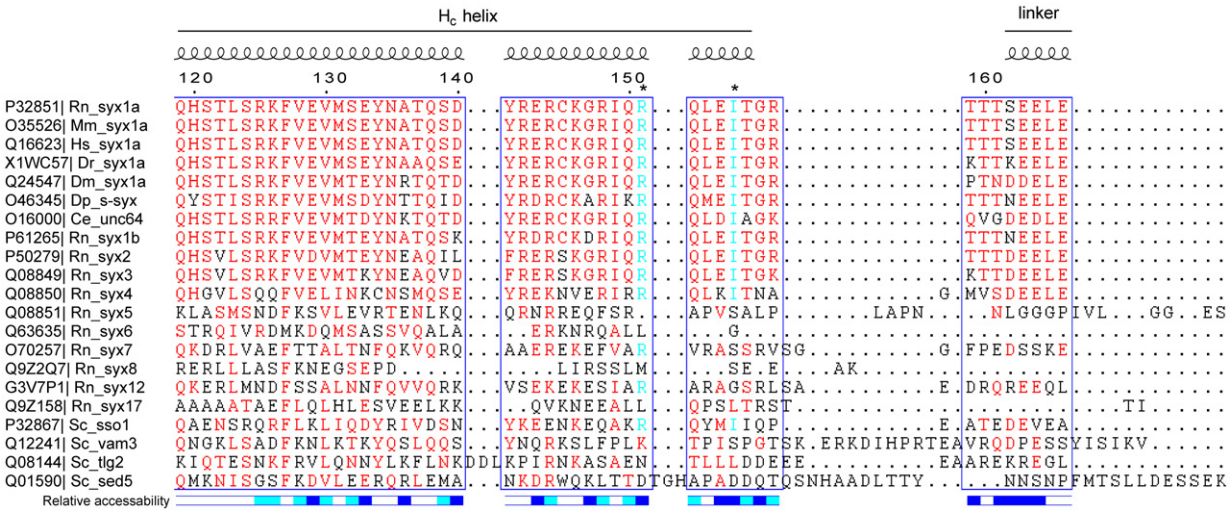

Figure EV3. Sequence alignment of the syntaxin-1 linker region.

Sequence alignment was performed with Clustal Omega and interpreted with ESPript 3.0. Residues above 60% similarity are colored in red, and residues R151 and I155 are colored in cyan and indicated by asterisks on the top of the sequences. Secondary structure and relative solvent accessibility were calculated based on the crystal structure of the Munc18-1/syntaxin-1 complex (PDB entry 3C98): white, buried; blue, exposed; cyan, partially exposed. UniProt entries of each of the sequences are on the left. Rn, *Rattus norvegicus*; Mm, *Mus musculus*; Hs, *Homo sapiens*; Dr, *Danio rerio*; Dm, *Drosophila melanogaster*; Dp, *Doryteuthis pealeii*; Ce, *Caenorhabditis elegans*; Sc, *Saccharomyces cerevisiae*.

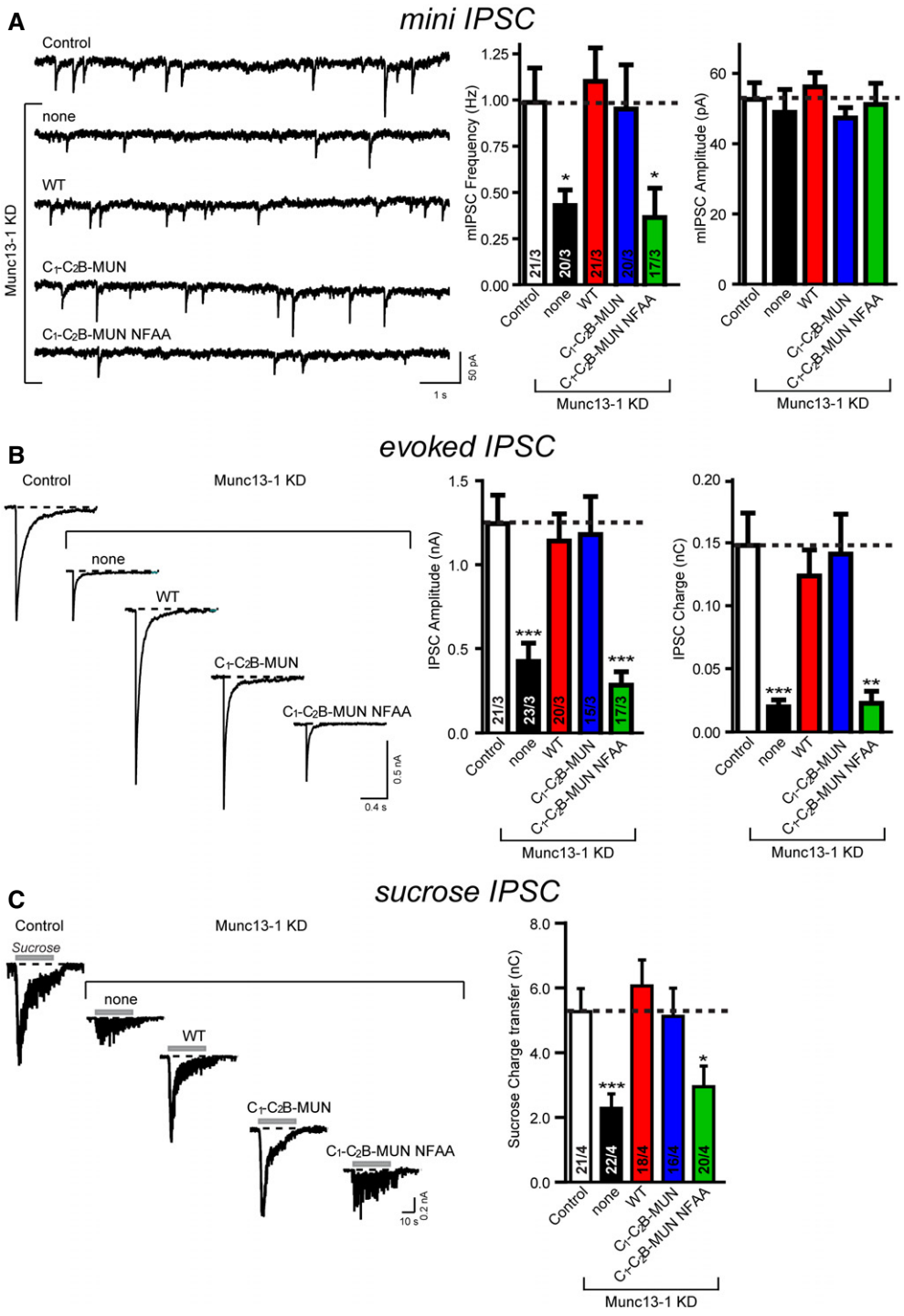

Figure EV4. The NF residues in the MUN domain of Munc13-1 are critical for synaptic vesicle priming and neurotransmitter release.

A Sample traces (left) and summary graphs (right) of mIPSCs recorded in WT hippocampal neurons that were infected with a control lentivirus (Control) or a lentivirus expressing only Munc13-1 shRNAs (none) or Munc13-1 shRNAs plus either full-length Munc13-1 (WT), or the C_1-C_2B-MUN fragment (C_1-C_2B-MUN) or the C_1-C_2B-MUN fragment containing the NFAA (N1128A, F1131A) mutations (C_1-C_2B-MUN NFAA), respectively.

B Sample traces (left) and summary graphs (right) of action potential-evoked IPSCs recorded in the infected neuronal cultures described in panel (A).

C Sample traces (left) and summary graphs (right) of IPSCs evoked by 0.5 M sucrose, recorded in the infected neuronal cultures described in panel (A).

Data information: Shown are means ± SEM; numbers of cells/independent cultures analyzed are listed in the bars. Statistical assessments were performed by Student's *t*-test comparing each condition to control (*$P < 0.05$; **$P < 0.01$; ***$P < 0.001$).

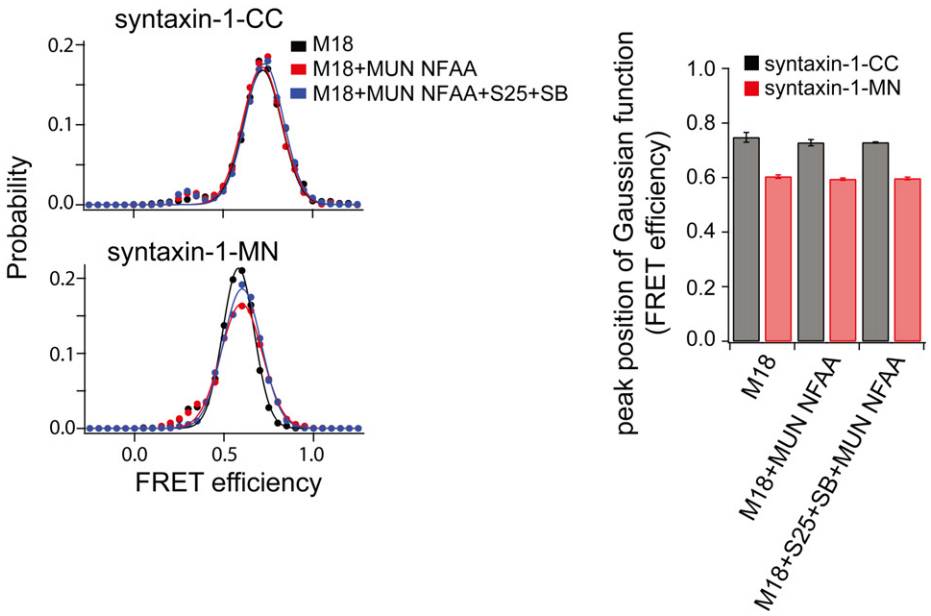

Figure EV5. Effect of the MUN domain containing the NFAA (N1128A, F1131A) mutations on conformational changes of syntaxin-1 bound to Munc18-1.
smFRET efficiency histograms and FRET efficiency values (bar chart) corresponding to the peak positions of the Gaussian functions fit to the smFRET efficiency histograms for the specified syntaxin-1 label pairs and conditions, using the same procedure as in Fig 4. The bar charts show mean values ± SD for the two subsets of an equal partition of the data that are comprised of the observed FRET efficiency values for all molecules in each different condition (see Appendix Tables S2 and S3). Shown are smFRET efficiency histograms for the cytoplasmic domain of syntaxin-1 bound to Munc18-1, upon the addition of the NFAA mutant of the MUN domain, upon the simultaneous addition of SNAP-25, the cytoplasmic domain of synaptobrevin-2, and the NFAA mutant of the MUN domain. S25, SNAP-25; SB, synaptobrevin-2; M18, Munc18-1.